

State and Topology Estimation for Unobservable Distribution Systems using Deep Neural Networks

B. Azimian, *Student Member, IEEE*, R. Sen Biswas, *Student Member, IEEE*, A. Pal, *Senior Member, IEEE*, Lang Tong, *Fellow, IEEE*, and Gautam Dasarathy, *Member, IEEE*

Abstract— Time-synchronized state estimation for reconfigurable distribution networks is challenging because of limited real-time observability. This paper addresses this challenge by formulating a deep learning (DL)-based approach for topology identification (TI) and unbalanced three-phase distribution system state estimation (DSSE). Two deep neural networks (DNNs) are trained to operate in a sequential manner for implementing DNN-based TI and DSSE for systems that are incompletely observed by synchrophasor measurement devices (SMDs). A data-driven approach for judicious measurement selection to facilitate reliable TI and DSSE is also provided. Robustness of the proposed methodology is demonstrated by considering realistic measurement error models for SMDs as well as presence of renewable energy. A comparative study of the DNN-based DSSE with classical linear state estimation (LSE) indicates that the DL-based approach gives better accuracy with a significantly smaller number of SMDs.

Index Terms— Deep neural network (DNN), State estimation, Synchrophasor measurements, Topology identification.

I. INTRODUCTION

Real-time monitoring and control of distribution networks was traditionally deemed unnecessary because it had radial configuration, unidirectional power flows, and predictable load patterns. However, the fast growth of behind-the-meter (BTM) generation, particularly solar photovoltaic (PV), electric vehicles, and storage, is transitioning the distribution system from a passive load-serving entity to an active market-ready entity, whose reliable and secure operation necessitates real-time situational awareness [1]-[2]. Phasor measurement units (PMUs), D-PMUs, and micro-PMUs, collectively referred to as synchrophasor measurement devices (SMDs) in this paper, have been introduced into the distribution system to provide fast (sub-second) situational awareness by enabling time-synchronized state estimation [3]-[4]. However, the number of SMDs in a typical distribution network are not large enough to provide an *independent* assessment of the system state. The assumption of Gaussian noise in synchrophasor measurements has also been disproved recently [5].

At the same time, modern distribution systems are being equipped with advanced metering infrastructure (AMI) in the

form of smart meters. By the end of 2018, 86.8 million smart meters had been installed in the U.S. alone [6]. Hence, prior research has combined smart meter data with SMD data for facilitating distribution system state estimation (DSSE) [7]. However, smart meters measure energy consumption from 15 minute to hourly time intervals and report their readings after a few hours or even a few days [8]. These two aspects make smart meter measurements unsuitable for real-time DSSE. Moreover, smart meter measurements are not time-synchronized, which makes their direct integration with SMD measurements a statistical challenge.

There have been quite a few recent papers that have proposed the use of machine learning (ML), in general, and neural networks, in particular, for performing DSSE. In [9], a shallow physics-aware neural network was used to implement DSSE. However, the approach did not consider the different time resolutions of smart meters, SMDs, and supervisory control and data acquisition (SCADA) data. In [10], an artificial neural network framework was used for three-phase unbalanced DSSE. The approach split the grid into multiple areas to improve DSSE accuracy as well as training time. However, smart meter measurements were not considered in the analysis (only micro-PMU measurements were used) and loads were varied by a Gaussian distribution which might not correctly represent the system behavior. In [11], a Bayesian approach was utilized for DSSE by training a deep neural network (DNN) to approximate the conditional mean of the joint probability distribution of the system states and measurements, both of which were treated as random variables. However, the approach was not validated for unbalanced three-phase distribution systems and non-Gaussian measurement noise. Furthermore, in [9]-[11], the topology of the system was assumed to be fixed.

As topology of a distribution network changes with time, it is important to account for it in the DSSE formulation [12]. In [13], a mixed integer linear programming approach was devised for estimating topology of distribution networks. The methodology required real-time measurements from line flow meters as well as smart meters. However, in most distribution systems it is still not possible to ping all the smart meters in real-time. In addition, the line flow meters were placed randomly, and the topology estimation was not integrated with DSSE. In [14], a graph-based optimization framework was proposed to recover topology of radial distribution networks using limited number of real-time meters. However, meshed grids and unbalanced multiphase distribution systems were not considered in the study. In [15], a data-driven physical probabilistic network model was used for topology recognition. However, the method relied on smart meter data which made it unsuitable for real-time knowledge of the network topology. In

This work was supported in part by the Advanced Research Projects Agency-Energy (ARPA-E) under award number DE-AR00001858-1631, by the Power Systems Engineering Research Center (PSERC) Grant T-63, and by the National Science Foundation (NSF) under the award OAC-1934766.

B. Azimian, R. Sen Biswas, A. Pal, and G. Dasarathy are with the School of Electrical, Computer and Energy Engineering, Arizona State University, Tempe, AZ, 85287, USA (e-mail: bazimian@asu.edu; rsenbisw@asu.edu; apal12@asu.edu; gautamd@asu.edu)

L. Tong is with the School of Electrical and Computer Engineering, Cornell University, Ithaca, NY 14850, USA (e-mail: lt35@cornell.edu)

[16], a time-series signature verification method was used to track topology changes from streaming micro-PMU measurements. One switching at a time and prior information of the switch status were two assumptions that limited the usefulness of this method. To summarize, a strategy for reliably performing ML-based DSSE during topology changes has not been investigated yet. This paper addresses this knowledge gap by making the following salient contributions:

1. A DNN-based topology identification (TI) is proposed to *estimate switch statuses in real-time* from sparsely placed SMDs.
2. A DNN-based DSSE for *unbalanced three-phase* distribution networks is developed that estimates states (voltage phasors) in a fast, time-synchronized manner.
3. Transfer learning is employed to account for the effects of *topology changes* on DSSE accuracy.
4. A judicious approach for *measurement selection* inside a DNN framework to facilitate reliable TI and fast time-synchronized DSSE is presented.
5. Robustness of the proposed method is demonstrated by considering *realistic errors* in SMD measurements.

II. THEORETICAL BACKGROUND AND PROPOSED APPROACH

A. Need for an ML-based DSSE

Time-synchronized state estimation in distribution networks using classical approaches, such as least-squares, requires the system to be completely observed by SMDs. However, it is highly unlikely that, at least in the near future, a distribution system will be equipped with as many SMDs as is required for complete observability. To circumvent the problem of scarcity of SMDs for doing time-synchronized DSSE, a Bayesian approach is formulated in this paper in which the state, x , and the measurement, z , are treated as random variables. Similar to [11], we create a minimum mean squared error (MMSE) estimator to minimize the estimation error as shown below.

$$\min_{\hat{x}(\cdot)} \mathbb{E}(\|x - \hat{x}(z)\|^2) \Rightarrow \hat{x}^*(z) = \mathbb{E}(x|z) \quad (1)$$

The MMSE estimator directly minimizes the estimation error while classical estimators, such as least-squares, minimize the modeling error embedded via the measurement function $h(\cdot)$ that relates the measurements with the states. By circumventing the need for $h(\cdot)$, the observability requirements get bypassed in a Bayesian state estimator. However, in (1), there are two underlying challenges to computing the conditional mean. First, the conditional expectation, which is defined by,

$$\mathbb{E}(x|z) = \int_{-\infty}^{+\infty} xp(x|z)dx \quad (2)$$

requires the knowledge of joint probability density function (PDF) between x and z , denoted by $p(x, z)$. When the number of SMDs are scarce, the PDF between SMD measurements and all the voltage phasors is unknown or impossible to specify, making the direct computation of $\hat{x}^*(z)$ intractable. Secondly, even if the underlying joint PDF is known, finding a closed-form solution for (2) can be difficult. A DNN is used in this paper to approximate the MMSE state estimator.

B. Sample Generation and Distribution Learning

As mentioned in Section I, smart meter measurements become available after a delay of at least a few hours, implying

that these measurements cannot be directly used for real-time DSSE. Therefore, the proposed methodology uses the historical slow timescale smart meter readings in the offline training process of the DNNs. The online stage only needs data from limited SMDs to carry out DSSE in real-time. In the offline stage, the smart meter energy readings are converted to average power by dividing the energy with the corresponding time interval. Then, the aggregated net injection at the distribution transformer level is calculated by summing up the readings of the smart meters connected to the transformer. The net load at each transformer is treated as a random variable.

Next, a *kernel density estimator* (KDE) is used to learn the distribution of aggregated smart meter readings. Although KDE is suitable for learning the PDF of data samples which do not exactly follow a parametric PDF, it is prone to overfitting which causes loss of generality of the fitted PDF [17]. We modify the KDE by adjusting its bandwidth to achieve 95% confidence interval ensuring that the fitted PDF effectively represents load behavior. After the PDF of active power injection is obtained, the reactive power is computed by selecting a power factor from a uniform distribution lying between 0.95 and 1. Monte Carlo (MC) sampling is done next to pick active and reactive power injections from the learnt distribution to run a large number of power flows. The voltage and current phasors obtained from the solved power flows are stored in the training database.

C. Deep Learning (DL)-based DSSE using DNN

According to the universal approximation theorem [18], a neural network is capable of approximating any arbitrary continuous function. Considering the fact that the MMSE estimator is a regression problem with the regressor, x , it can be implied that the MMSE estimator in (1) can be approximated by a sufficiently large DNN that can capture the non-linearities and complexities of the distribution system such as unbalanced loads, varying regulator taps and capacitor banks, and incomplete observability for different operating conditions. Consequently, a Bayesian DSSE is implemented by training a regression DNN offline, and then using the trained DNN during real-time operation to estimate the states. The inputs to the DNN are the z obtained from SMDs and the outputs are the estimated voltage phasors, $\hat{x}^*(z)$.

The proposed DNN structure is shown in Figure 1. In this figure, m is the total number of measurements available from SMDs, n is the total number of states, a denotes the activation function, b denotes the bias, and W refers to the weights conveying the output of previous neurons to the neurons of the next layer. Dropout is also applied to avoid overfitting. Note that for an incompletely observed distribution network, $n \gg m$. The number of neurons and hidden layers are hyper-parameters that must be tuned offline. The rectified linear unit (ReLU) activation function is used for the hidden layers, while a linear activation function is used for the output layer. The loss function is chosen to be the empirical mean-square error which is consistent with the Bayesian approach. During the offline training process the weights are optimized to minimize the mean squared error using the backpropagation algorithm [19]. In real-time operation, SMD data is fed into the trained feed forward DNN and the estimated state, \hat{x}^* , is obtained.

The unique aspects of SMDs and distribution networks are also considered in this study. An SMD typically has six

channels which measures three nodal voltage phasors and three branch current phasors [3]-[4]. This provides observability of individual phases at the node equipped with the SMD. Each phasor magnitude and angle are separate features that are fed into the input layer of the DNN. The voltage magnitude and angle of every phase of every node is estimated at the output layer. The salient characteristics of a distribution network such as wye-delta loads, zero-injection phases, voltage regulators, transformers, and capacitor banks are included in the physical network model used for creating the samples for DNN training.

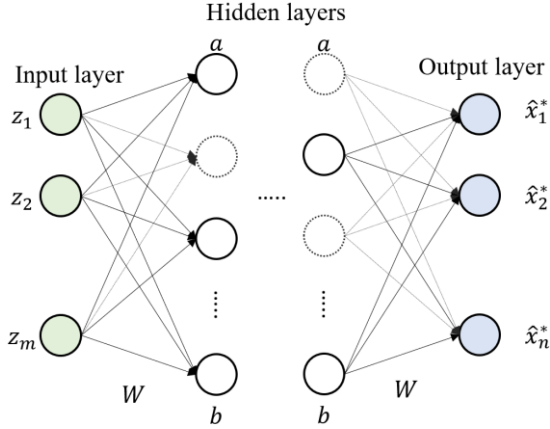


Figure 1: DNN structure for DNN-based DSSE with dropout

D. DL-based Topology Identification (TI) and Transfer Learning

When a topology change occurs, the DNN for DSSE trained for the old topology will receive test data from another feature space that corresponds to the new topology. As this might lower the performance of the DNN for DSSE, a sequential procedure is adopted in this paper in which the new topology is identified first and the DNN for DSSE is updated afterwards based on the identified (new) topology.

TI is a challenging task for distribution networks because the switch statuses are usually not monitored in real-time. To overcome this problem, we train a classification DNN for TI that uses measurements from sparsely placed SMDs. In the DNN for TI, the number of neurons in the output layer is equal to the number of *feasible* topologies in the network, the SoftMax function is used as the activation function for the output layer, while the categorical cross-entropy is chosen to be the loss function (the inputs and activation function for the hidden layers are the same as the DNN for DSSE). Here, feasible topologies refer to those switch configurations for which the system does not split into islanded sub-systems. For training the DNN for TI, the database generation process (see Section II.B) is repeated for all feasible topologies. A distinct advantage of the proposed DNN-based TI is that it only requires high-speed time-synchronized SMD measurements for online operation as opposed to [13], [15], which needed smart meter measurements in real-time. This implies that the proposed topology processor can run at SMD timescales.

For updating the DNN for DSSE, two possibilities exist. One option is to train the DNN for DSSE afresh for the new topology. However, doing so may take a very long time. An alternate (better) solution is to use *Transfer learning* to transfer the knowledge gained from the old topology to the new topology [20]. Transfer learning tries to improve the learning of

the target prediction function in the target domain using the knowledge available in the source domain and task. A domain \mathcal{D} comprises two parts: a feature space \mathcal{Z} and a marginal probability distribution $P(z)$. Given \mathcal{D} , a task \mathcal{T} comprises two parts: a label space \mathcal{X} and an objective prediction function $\mathcal{K}(\cdot)$. In DNN-based DSSE under varying topologies, the feature space \mathcal{Z} does not change as the same SMD measurements will be used for different topologies. However, the marginal probability distribution functions, $P(z)$, do change because loads must be served by different paths when topology changes. i.e., $\mathcal{D}_s \neq \mathcal{D}_T$. Similarly, the label space \mathcal{X} does not change because the number of states (i.e., voltage phasor at each node) and their nature does not change. However, the prediction function, $\mathcal{K}(\cdot)$, namely, the regression DNN model, must be retrained for the target domain, i.e., $\mathcal{T}_s \neq \mathcal{T}_T$. In accordance with this problem set-up, *inductive Transfer learning* [21] is applied to induce transfer of knowledge gained from \mathcal{D}_s and \mathcal{T}_s (old topology) to \mathcal{D}_T and \mathcal{T}_T (new topology).

Four approaches have been proposed for implementing inductive Transfer learning: feature-representation transfer, instance transfer, relational-knowledge transfer, and parameter transfer [22]. Here we use *parameter transfer* to update the DNN for DSSE as its (DNN's) parameters can be used for multiple domains. Two well-known parameter-based transfer learning methods are parameter-sharing and fine-tuning. Parameter-sharing assumes that the parameters are highly transferable due to which the parameters in the source domain can be directly copied to the target domain, where they are kept "frozen". Fine-tuning assumes that the parameters in the source domain are useful, but they must be trained with limited target domain data to better adapt to the target domain [23]. Since there is no guarantee that the parameters of the DNN-based DSSE will be highly transferable for all feasible topologies, *fine-tuning* is used in this paper to update the weights of the DNN for DSSE when topology changes (see Section IV.C for implementation of the proposed methodology).

III. MEASUREMENT SELECTION

An integrated framework is proposed here to identify suitable locations for placing SMDs for performing DNN-based TI and DSSE. Since it is crucial to know the network model before doing DSSE, TI must be performed first to estimate the current network topology. Hence, we initially find the locations for accurate TI (Section III.A). If those locations do not satisfy the criteria for measurement selection for DNN-based DSSE, we find additional locations where SMDs can be placed (Section III.B). An overview of the integrated measurement selection algorithm is provided in Figure 2.

A. Measurement selection for DNN-based TI

DNN-based TI is a classification problem in which we estimate the topology of the system, i.e., the status of all the switches, from SMD measurements. Hence, measurement selection for DNN-based TI can be viewed as a feature selection problem, whose objective is to find the suitable location of SMDs required to achieve acceptable TI performance. Current phasors (in contrast to voltage phasors) are used for training the DNN classifier as opening/closing the switches will have a bigger influence on the currents flowing through the network.

Sequential forward selection, a greedy search algorithm that starts with an empty set and adds features based on the criterion of ML classifier accuracy [24], is used to determine the appropriate current phasor measurements. The number of desired features is a hyper-parameter that is tuned to find the minimum number of features for a given accuracy level. For example, if at least $\alpha\%$ accuracy is desired, then the number of desired features will be increased gradually until an accuracy of $\alpha\%$ is reached. It is very difficult to find which input features of a DNN have the most significant impact on the output variables as each input feature goes through several hidden layers and the sensitivity of each output neuron to the input features may become difficult to compute [25]. However, sequential forward selection can be easily done with other ML techniques, such as, support vector machines. Hence, we first run sequential forward selection algorithm on a support vector classifier and then we use the selected features for training the DNN for TI.

B. Measurement selection for DNN-based DSSE

DNN-based DSSE is a regression problem for which all voltages and currents of the distribution network can be potential input features. The most common technique for finding the best features for a regression problem is by using correlation coefficients [26]. In this paper, we use *Spearman's correlation coefficient* computed using the voltage phasors for feature selection for DNN-based DSSE. It was observed that the presence of transformers and multiple outgoing laterals from the feeder head splits the correlation coefficient matrix into multiple clusters. We placed one SMD in every identified cluster as adding more SMDs to the same cluster will not improve DNN performance because features in the same cluster are rank correlated, and hence likely to not provide extra information. Among the nodes that belong to the same cluster, the SMD was placed at the location that maximized observability. In this context, a metric called the phase observability index (POI), based on the bus observability index (BOI) of [27], and defined as the *total number of phase voltages observed from a given node*, was used to screen out the locations for SMD installation.

IV. DATA CONSIDERATION AND METHODOLOGY OVERVIEW

A. Two level Error Model for SMDs

According to the IEEE Standard [28], SMDs should meet the total vector error (TVE) requirement of 1%. It has also been widely assumed that the errors in SMD data follow a Gaussian distribution [29]. However, SMDs are connected to the grid through an instrumentation channel consisting of instrument transformers, cables, and burden. These components not only cause the total measurement error to go beyond the 1% TVE limit, but also change the shape of the error distribution, e.g., from a Gaussian to a 3-component Gaussian mixture model (GMM) [5]. Note that the instrument transformer error alone for voltage magnitudes, voltage angles, current magnitudes, and current angles can be as high as $\pm 1.2\%$, $\pm 1^\circ$, $\pm 2.4\%$ and $\pm 2^\circ$, respectively [30]. To account for these practical constraints, a two-level error model was introduced in [31], which is also used here. In the first level, the instrumentation channel error is modeled by a 3-component GMM with the corresponding magnitude and angle errors added to the true voltages and

currents. In the next level, a Gaussian TVE is added to the previously obtained erroneous measurements. This two-level error model ensures the generation of realistic SMD data.

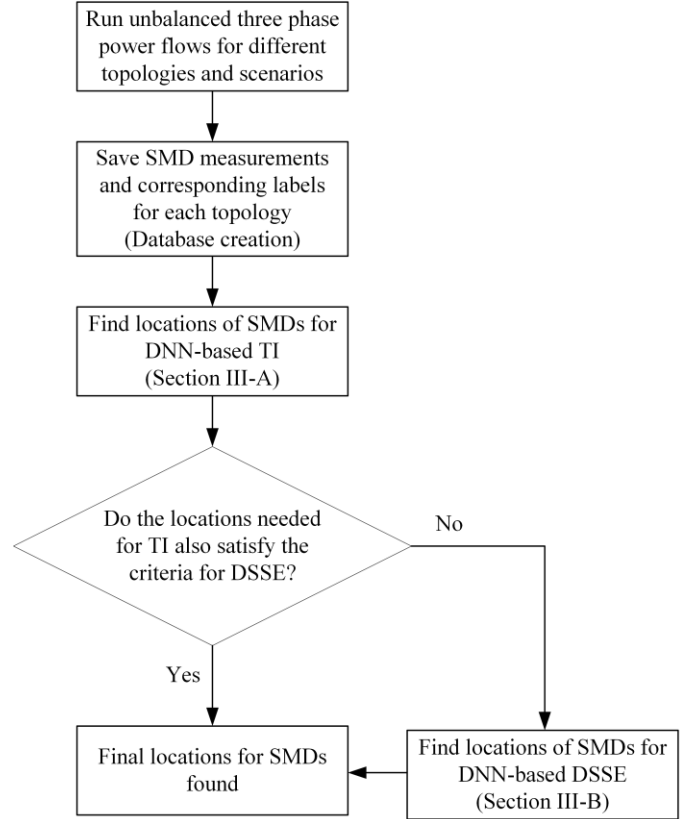


Figure 2: Integrated SMD placement for DNN-based TI and DSSE

B. Errors in smart meter measurements

Energy readings obtained from smart meters are also prone to measurement errors. For example, the magnitude of the error in energy readings can be as high as 10% and can be reasonably well-represented by a normal distribution [32]. However, the impact of erroneous smart meter measurements on the performance of the proposed DNN-based TI and DSSE is different from the impact of SMD measurement errors. This is because smart meter data is utilized to create PDFs of different loading conditions and not directly employed in DNN training. It is the random samples drawn from the PDFs that are fed into the power flow solver to generate voltages and currents, which are then used for learning the relation between SMD measurements and states/topologies via the DNNs. Therefore, the impact of smart meter errors will be observed by checking the quality of the PDFs that are generated (see Section II.B). This was done by applying the *two-sample Kolmogorov-Smirnov (KS) test* to the true and erroneous smart meter measurements to check whether the two sets of data are from the same distribution or not. If the null hypothesis is not rejected for the true and erroneous smart meter data, then it means that the PDFs generated from erroneous measurements by KDE can be used for MC sampling and power flow calculation.

C. Implementation of DNN-based TI and DSSE

The procedure to be followed for implementing the proposed methodology is presented in Figure 3. The model is split into an offline learning stage and a real-time operation stage.

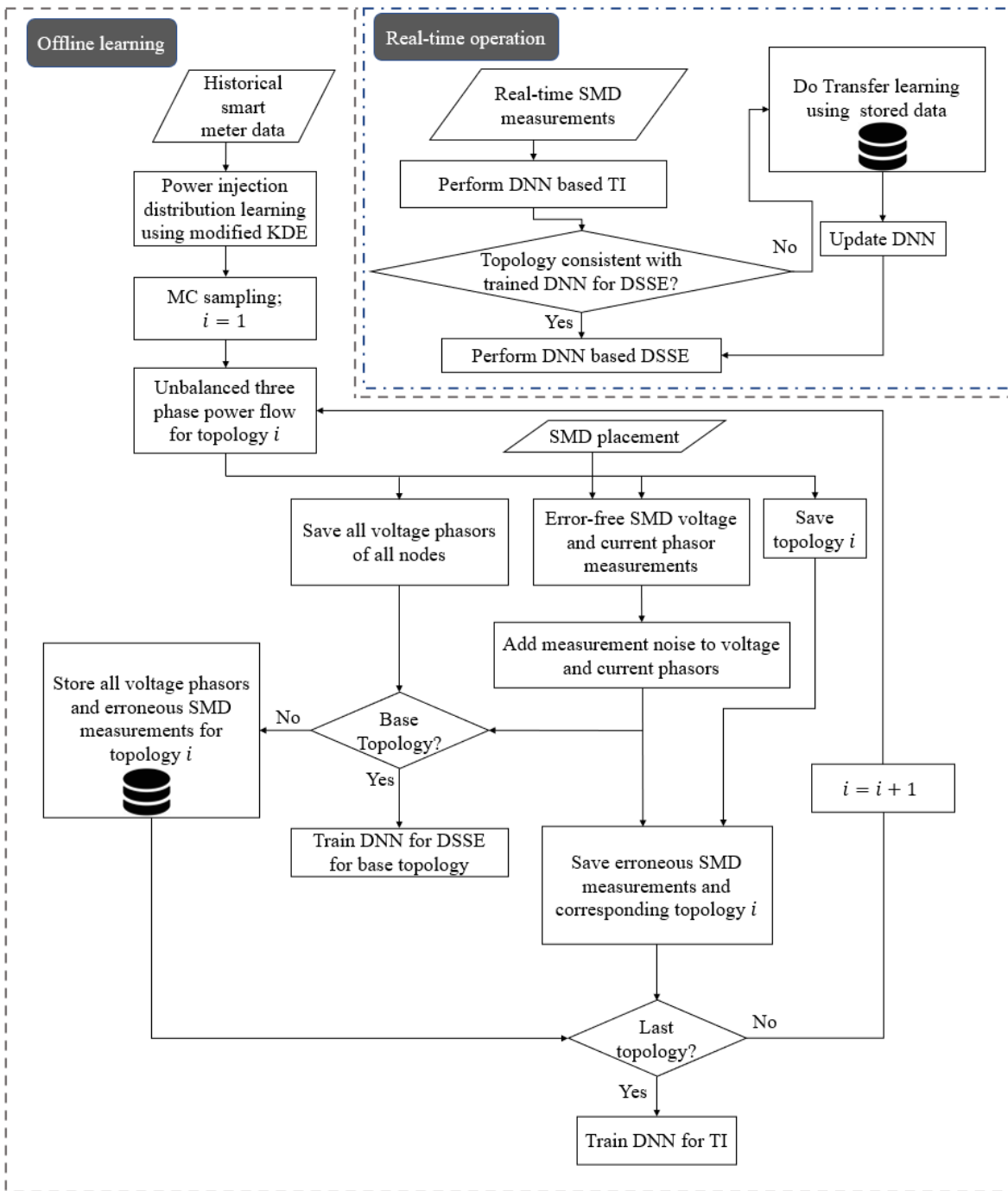


Figure 3: Implementation of the proposed DNN-based TI and DSSE

1) Offline learning

In the offline learning stage, historical smart meter data is used to find the PDFs of the power injections at a given node. MC sampling of power injections is done from the best-fit PDF to run three-phase unbalanced power flows. The voltage phasors, SMD measurements, and topology information is saved for each solved power flow. For the current configuration of the system (called base topology), a DNN is trained for performing DSSE. For other network configurations, all voltage phasors and SMD data are saved for each feasible topology. Once the data from power flow results are saved for all feasible topologies, a separate DNN is trained for performing TI.

2) Real-time operation

For real-time operation, the trained DNN-based TI is used to estimate the current network topology from real-time SMD data. If the estimated topology is consistent with the base topology, the DNN trained for the base topology is employed to perform DSSE. If the estimated topology is different from the base topology, Transfer learning (using fine-tuning) is employed to update the DNN used for performing DSSE, and the current topology becomes the new base topology. Essentially, fine-tuning provides a more effective initialization (than random initialization) by using the weights from the previously well-trained DNN. By doing this, it bypasses the need for large amounts of data (and time) for DNN re-training.

V. SIMULATION RESULTS

A. Simulation Settings

1) Distribution system setup

Simulations are performed on the IEEE 34-node system (System S1) [33] and a 240-node distribution network of Midwest U.S. (System S2) [34]. In System S1, three distributed generation (DG) units having ratings of 300kW, 600kW, and 1MW are placed on nodes 816, 836, and 890, respectively, to model the effect of renewable generation. The loads and DG units are varied by 50% to create different scenarios for this system. System S2 has smart meters installed at all customer premises and has all the characteristics of a modern distribution network, namely, underground and overhead lines, capacitors and regulators, single, double, and three-phase laterals and loads. One-year of smart meter readings is also available for this system. PDFs (computed using KDE) were fit to the historical hourly smart meter data, while ensuring that there was no overfitting. Network models of Systems S1 and S2 are available in OpenDSS [35]. While performance of DNN-based DSSE is evaluated for both systems, DNN-based TI results is presented for System S2 only, as System S1 does not have any switches.

2) Neural network setup

Hyper-parameter tuning is the most crucial part of DNN training. The hyper-parameter information for the two DNNs are summarized in Table I. Keras v. 2.2.4 with TensorFlow v.2.1.0 as the back-end was used in Python v.3.7.7 to carry out the training. All simulations were performed on a computer with 64.0 GB RAM and Intel Core i7-8700k CPU @3.70GHz.

Table I: Hyper-parameters for DNN-based TI and DSSE

Hyper-parameters	DNN-based TI	DNN-based DSSE
No. of neurons in input layer	2×No. of measured phasors by all SMDs	2×No. of measured phasors by all SMDs
No. of neurons in each hidden layer	800	500
No. of hidden layers	5	5
No. of output neurons	No. of feasible topologies	No. of states
Hidden layer activation function	ReLU	ReLU
Output layer activation function	SoftMax	Linear
Initializer method	He normal	He normal
Optimizer	ADAM	ADAM
No. of epochs	50	200
No. of samples	1,000 per topology	12,500
Training percentages	80% training and validation, 20% testing	80% training and validation, 20% testing
Learning rate (lr)	0.1 with reduce lr on Plateau	0.1 with reduce lr on Plateau
Regularization	30% Dropout	30% Dropout
Loss function	Categorical cross-entropy	Mean squared error

B. IEEE 34-node system (System S1)

There are no switches present in System S1, so only measurement selection for DNN-based DSSE is required. On computing the Spearman's correlation coefficient, it was observed that System S1 can be split into two clusters: a smaller cluster comprising nodes 888 and 890, and a larger cluster, containing all the remaining nodes. Therefore, only two SMDs were needed for this system. Figure 4 shows the phase mean

absolute error (MAE) for DNN-based DSSE for four cases. Case (a): one SMD is placed inside the large cluster at a location (808-812) that has high POI (red dots). Case (b): one SMD is placed in the small cluster at a location (888-890) that has high POI (blue cross). Case (c): two SMDs are placed at two locations (808-812 and 830-854) that have high POI but are in the same (large) cluster (black cross). Case (d): two SMDs are placed at two locations (808-812 and 888-890) that have high POI but are in different clusters (blue dots). Note that a location $i - j$ means that the SMD monitors the voltage at node i and the currents flowing from node i to node j . From Figure 4, it is clear that the MAE decreased considerably when the two SMDs were placed in two different clusters (Case (d)), which is consistent with the logic proposed in Section III.B.

Next, the performance of DNN-based DSSE is compared with the classical linear state estimation (LSE) [36]; the results are shown in Table II. To satisfy LSE's complete observability requirement, System S1 needed 26 SMDs (based on the optimization framework proposed in [37]). It can be observed from Table II that DNN-based DSSE outperforms classical LSE in terms of both phase MAE and magnitude mean absolute percentage error (MAPE) with only *two* SMDs. Furthermore, to give confidence to the outputs of the DNN, the *tolerance interval* was computed. Tolerance interval provides the upper and/or lower bounds within which, with some confidence level, a specified proportion of the samples fall [38]. In this study, the confidence level and population proportion were both set at 95%. We use the upper bound of the tolerance interval as a measure of the confidence of the state estimates. In reference to Table II, 0.3° tolerance interval for voltage angles implies that with confidence level of 95%, 95% of the error values in estimating the angles by the DNN-based DSSE were less than 0.3°. Note that for comparing the DNN-based DSSE results with LSE, the GMM error was removed from the data generation process of LSE and only 1% TVE for SMDs was considered. This is because the least-squares-based LSE is guaranteed to give the best possible result in situations where the measurement noise follows a Gaussian distribution. Lastly, it was observed that the proposed DNN-based DSSE was robust to the error model of the data as its performance deteriorated negligibly when the two-level error model was used instead.

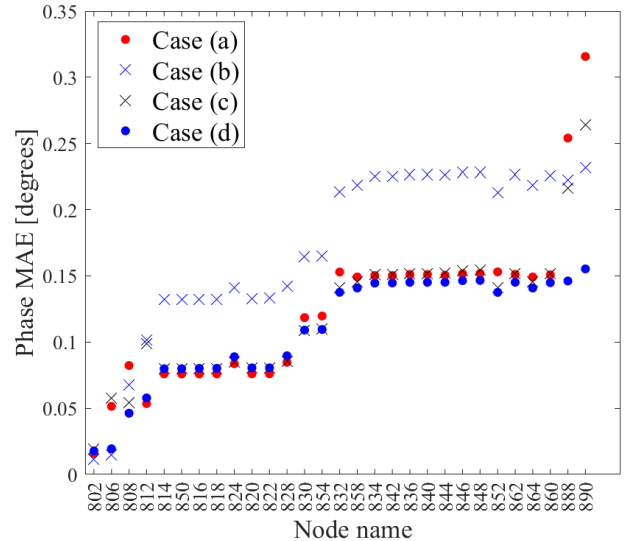


Figure 4: Phase angle MAE for DNN-based DSSE for System S1

Table II: Comparing the performance of DNN-based DSSE with classical LSE for System S1

Method	Error model	Phase error [degrees]		Magnitude error [%]		# SMD
		MAE	Tolerance interval	MAPE	Tolerance interval	
LSE	1% Gaussian TVE	0.14	0.4	0.25	0.6	26
DNN-based DSSE	1% Gaussian TVE	0.09	0.3	0.18	0.5	2
DNN-based DSSE	Two-level GMM	0.11	0.3	0.20	0.6	2

C. 240-node distribution network of Midwest US (System S2)

1) DNN-based TI and DSSE

Due to switches being present in System S2, SMD placement for TI was done first based on the integrated measurement selection algorithm (see Section III). Considering the locations of the 9 switches (see Figure 5), 84 feasible topologies were identified. 1,000 samples were generated by varying the loads for each of the 84 topologies. The two-sample KS test was also done after adding 10% noise to the historical smart meter data, and it was verified that the null hypothesis was not rejected for any of the loads. Based on the sequential forward selection algorithm, four SMDs were placed at 1010-2057, 2012-2013, 2021-2026, and 3030-3031 to attain an accuracy of 99.19% for TI. The locations are depicted in Figure 5.

Measurement selection for DNN-based DSSE using the Spearman's correlation coefficient was investigated next. It was observed that based on this metric, System S2 could be split into two clusters: one comprising Feeders A and B, and one

comprising Feeder C; implying that at least two SMDs would be required. However, four SMDs (= one in Feeder A, two in Feeder B, and one in Feeder C) had already been placed in this system based on the measurement selection algorithm for DNN for TI. As these four SMDs satisfied the requirements for DNN-based DSSE, no additional SMDs were placed in this system.

The performance of DNN-based DSSE was now compared with the classical LSE for System S2. The total number of SMDs required for complete observability of System S2 was 113 (based on the optimization framework proposed in [37]). It can be observed from Table III that the DNN-based DSSE outperforms classical LSE with only *four* SMDs. Moreover, the accuracy of DNN-based DSSE is practically the same with 1% Gaussian TVE and with the two level-GMM error model, confirming that the DNN-based DSSE is robust against both the error model and the error magnitude.

2) Transfer learning for different network topologies

When topology changes occur, after correctly identifying the new topology using DNN-based TI, the DNN trained for doing DSSE for the old topology, must be updated. As mentioned in Figure 3, the TI and DSSE work sequentially and Transfer learning is used to update the DNN for DSSE after the topology of the system has changed. Two scenarios are considered below to show the applicability of the proposed methodology. In Scenario 1, the system is initially operating in the base topology (T1). Then, configurations of multiple switches are changed to create a new topology (T2), and afterwards, the system reverts back to its base topology (T1). In Scenario 2, the first and second topology changes are similar to Scenario 1, but in the third step, T2 changes to another topology (T3) which is different from both T2 and T1. The summary of network reconfigurations for both scenarios are shown in Table IV.

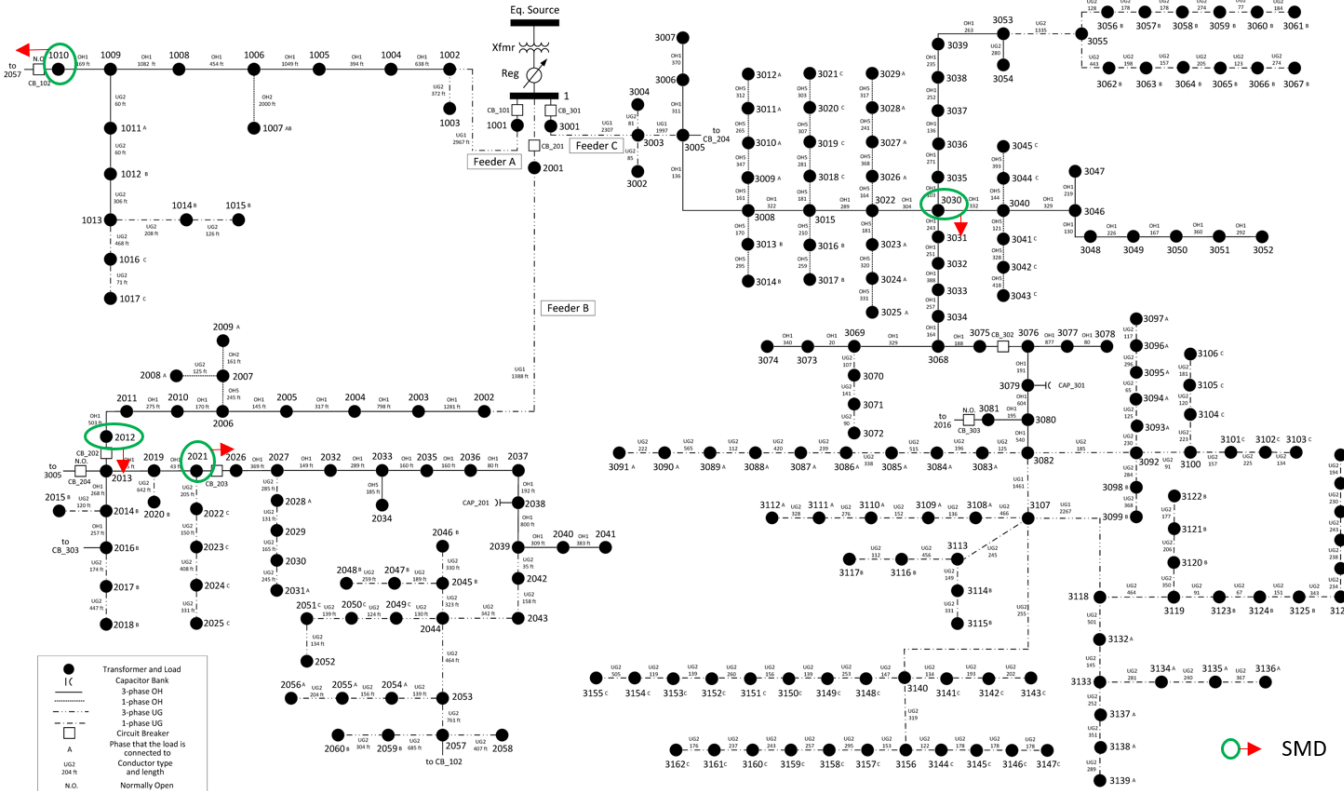


Figure 5: System S2 with SMD locations

Table III: Comparing the performance of DNN-based DSSE with classical LSE for System S2

Method	Error model	Phase error [degrees]		Magnitude error [%]		# SMD
		MAE	Tolerance interval	MAPE	Tolerance interval	
LSE	1% Gaussian TVE	0.14	0.35	0.25	0.61	113
DNN-based DSSE	1% Gaussian TVE	0.04	0.10	0.10	0.28	4
DNN-based DSSE	Two-level GMM	0.04	0.10	0.11	0.28	4

Table IV: Switch configurations for different scenarios

Switch name	Scenario 1			Scenario 2		
	T1	T2	T1	T1	T2	T3
CB_101	1	0	1	1	0	0
CB_102	0	1	0	0	1	1
CB_201	1	0	1	1	0	1
CB_202	1	1	1	1	1	1
CB_203	1	1	1	1	1	1
CB_204	0	1	0	0	1	0
CB_301	1	1	1	1	1	0
CB_302	1	0	1	1	0	1
CB_303	0	1	0	0	1	1

Figure 6 and Figure 7 present the results for Scenario 1 and Scenario 2, respectively. It can be seen from the plots that it takes only 8 seconds for the fine-tuning of the DNN, while complete training for a new topology would have needed 466 seconds. This is because 10,000 samples and 200 epochs are needed for training and validation of a completely new DNN for DSSE for a new topology (see Table I), while by taking advantage of fine-tuning only 1,000 samples and 10 epochs were needed, thereby reducing the training time significantly. This is an important result because if different switching events were to manifest every few minutes, then without Transfer learning we will not be able to achieve accurate DSSE results when it is needed most. Hence, this fast update of the DNN-based DSSE considerably improves the real-time monitoring capability of the proposed approach during switching events.

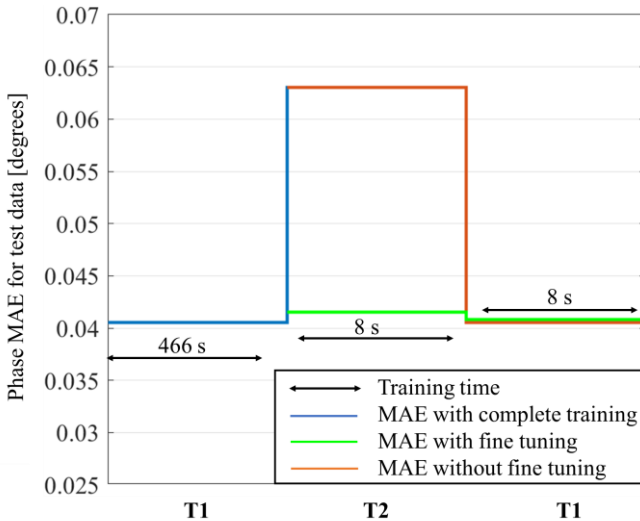


Figure 6: Comparative study of DNN-based DSSE for Scenario 1 with and without fine-tuning of the DNN by Transfer learning

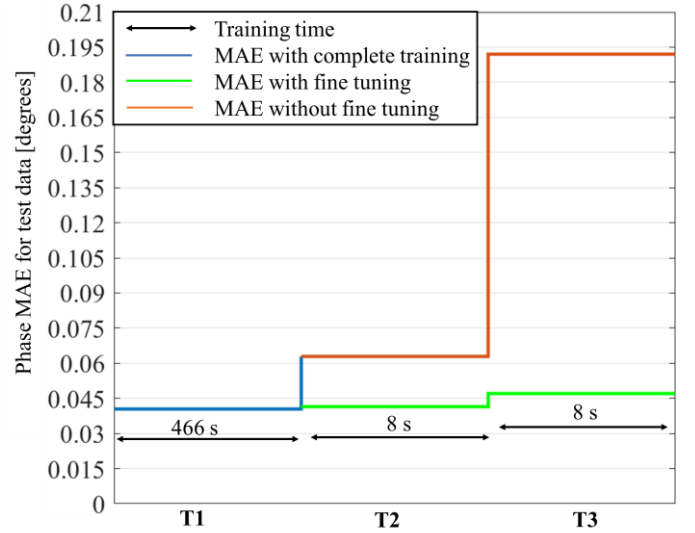


Figure 7: Comparative study of DNN-based DSSE for Scenario 2 with and without fine-tuning of the DNN by Transfer learning

The phase MAE results are now compared with and without fine-tuning of the DNN by Transfer learning. It is observed from Figure 6 and Figure 7 that if the old DNN was used for the new topologies, the error can increase by more than 1.5 times for the change from T1 to T2 and almost 4 times for the change from T2 to T3. Therefore, by using Transfer learning, DNN-based DSSE can be done quickly and accurately during varying network topologies.

VI. CONCLUSION

In this paper, a DNN framework for performing unbalanced three-phase time-synchronized DSSE for different network configurations is proposed that does not require complete observability of the network by SMDs. The unique feature of the proposed algorithm is that it can initially detect changes in network topology, and subsequently employ Transfer learning to update the DNN for DSSE in real-time for the new topology. Additionally, a structured methodology for measurement selection is proposed to enhance the performance of DNN-based DSSE for varying network configurations. The performance of the proposed DNN-based DSSE is validated by comparing it with the classical LSE. The simulation results on a renewable-rich IEEE 34-node distribution feeder and the 240-node Midwest U.S. system show that the proposed method: (1) can achieve better DSSE accuracy with a significantly lesser number of SMDs, (2) can efficiently detect varying network topologies for reconfigurable distribution systems, (3) ensures reliable DSSE for different topologies, and (4) is robust against non-Gaussian measurement noise and presence of renewable energy. The ability of the proposed algorithm to provide reliable state estimates with very few SMDs in large distribution networks for different topologies makes it a suitable candidate for enhanced monitoring and control of actual distribution systems.

REFERENCES

- [1] S. Singh, V. Babu Pamshetti, A. Thakur, and S. Singh, "Multistage multiobjective volt/var control for smart grid-enabled CVR with solar PV penetration", *IEEE Syst. J.*, pp. 1-12, May 2020.

- [2] S. Huang, Q. Wu, L. Cheng, and Z. Liu, "Optimal reconfiguration-based dynamic tariff for congestion management and line loss reduction in distribution networks," *IEEE Trans. Smart Grid*, vol. 7, no. 3, pp. 1295-1303, May 2016.
- [3] A. von Meier, E. Stewart, A. McEachern, M. Andersen, and L. Mehrmanesh, "Precision micro-synchrophasors for distribution systems: a summary of applications," *IEEE Trans. Smart Grid*, vol. 8, no. 6, pp. 2926-2936, Nov. 2017.
- [4] Z. Wu *et al.*, "Optimal PMU placement considering load loss and relaying in distribution networks," *IEEE Access*, vol. 6, pp. 33645-33653, 2018.
- [5] T. Ahmad, and N. Senroy, "Statistical characterization of PMU error for robust WAMS based analytics," *IEEE Trans. Power Syst.*, vol. 35, no. 2, pp. 920-928, Mar. 2020.
- [6] "U.S. Energy Information Administration (EIA)", *Eia.gov*, 2021. [Online]. Available: <https://www.eia.gov/tools/faqs/faq.php?id=108&t=3>. [Accessed: 23-Feb-2021].
- [7] P. A. Pegoraro, A. Meloni, L. Atzori, P. Castello, and S. Sulis, "PMU-based distribution system state estimation with adaptive accuracy exploiting local decision metrics and IoT paradigm," *IEEE Trans. Instrum. Meas.*, vol. 66, no. 4, pp. 704-714, Apr. 2017.
- [8] D. Zarrilli, A. Giannitrapani, S. Paoletti, and A. Vicino, "Energy storage operation for voltage control in distribution networks: a receding horizon approach," *IEEE Trans. Control Syst. Technol.*, vol. 26, no. 2, pp. 599-609, Mar. 2018.
- [9] A. S. Zamzam, and N. D. Sidiropoulos, "Physics-aware neural networks for distribution system state estimation," *IEEE Trans. Power Syst.*, vol. 35, no. 6, pp. 4347-4356, Nov. 2020.
- [10] B. Zargar, A. Angioni, F. Ponci, and A. Monti, "Multiarea parallel data-driven three-phase distribution system state estimation using synchrophasor measurements," *IEEE Trans. Instrumentation and Measurement*, vol. 69, no. 9, pp. 6186-6202, Sep. 2020.
- [11] K. R. Mestav, J. Luengo-Rozas, and L. Tong, "Bayesian state estimation for unobservable distribution systems via deep learning," *IEEE Trans. Power Syst.*, vol. 34, no. 6, pp. 4910-4920, Nov. 2019.
- [12] H. Wang, W. Zhang and Y. Liu, "A robust measurement placement method for active distribution system state estimation considering network reconfiguration," *IEEE Trans. Smart Grid*, vol. 9, no. 3, pp. 2108-2117, May 2018.
- [13] A. Gandluru, S. Poudel, and A. Dubey, "Joint estimation of operational topology and outages for unbalanced power distribution systems," *IEEE Trans. Power Syst.*, vol. 35, no. 1, pp. 605-617, Jan. 2020.
- [14] G. Cavarro, A. Bernstein, V. Kekatos, and Y. Zhang, "Real-time identifiability of power distribution network topologies with limited monitoring," *IEEE Control Syst. Letters*, vol. 4, no. 2, pp. 325-330, Apr. 2020.
- [15] W. Jiang *et al.*, "A physical probabilistic network model for distribution network topology recognition using smart meter data," *IEEE Trans. Smart Grid*, vol. 10, no. 6, pp. 6965-6973, Nov. 2019.
- [16] G. Cavarro and R. Arghandeh, "Power distribution network topology detection with time-series signature verification method," *IEEE Trans. Power Syst.*, vol. 33, no. 4, pp. 3500-3509, Jul. 2018.
- [17] M. Anneken, Y. Fischer and J. Beyerer, "Evaluation and comparison of anomaly detection algorithms in annotated datasets from the maritime domain," in *Proc. SAI Intelligent Systems Conf. (IntelliSys)*, London, UK, pp. 169-178, Dec. 2015.
- [18] S. Sonoda, and N. Murata, "Neural network with unbounded activation functions is universal approximator," *Appl. Comput. Harmon. Anal.*, vol. 43, no. 2, pp. 233-268, Sep. 2017.
- [19] I. Goodfellow, Y. Bengio, A. Courville, Y. Bengio, *Deep learning*, vol. 1. No. 2. Cambridge: MIT press, 2016. p. 200.
- [20] Y. Yang, Z. Yang, J. Yu, K. Xie, and L. Jin, "Fast economic dispatch in smart grids using deep learning: an active constraint screening approach," *IEEE Internet of Things J.*, vol. 7, no. 11, pp. 11030-11040, Nov. 2020.
- [21] S. J. Pan and Q. Yang, "A survey on transfer learning," *IEEE Trans. Knowledge Data Engineering*, vol. 22, no. 10, pp. 1345-1359, Oct. 2010.
- [22] S. Niu, Y. Liu, J. Wang and H. Song, "A decade survey of transfer learning (2010-2020)," *IEEE Trans. Artificial Intelligence*, vol. 1, no. 2, pp. 151-166, Oct. 2020.
- [23] Y. Zhang, Y. Zhang, and Q. Yang, "Parameter transfer unit for deep neural networks," *Advances in Knowledge Discovery and Data Mining*, Cham: Springer International Publishing, pp. 82-95, 2019.
- [24] T. Rückstieß, C. Osendorfer, and P. van der Smagt, *Sequential Feature Selection for Classification*. AI 2011: Advances in Artificial Intelligence, pp.132-141.
- [25] C. A. Jensen, M. A. El-Sharkawi and R. J. Marks, "Power system security assessment using neural networks: feature selection using Fisher discrimination," in *IEEE Transactions on Power Systems*, vol. 16, no. 4, pp. 757-763, Nov. 2001.
- [26] R. Alhalaseh, H. A. Tokel, S. Chakraborty, G. Alirezaei, and R. Mathar, "Feature-selection based PMU placement for detection of faults in power grids," in *Proc. 28th International Telecommunication Networks Applications Conference (ITNAC)*, Sydney, NSW, 2018, pp. 1-6.
- [27] D. Dua, S. Dambhare, R. K. Gajbhiye, and S. A. Soman, "Optimal multistage scheduling of PMU placement: an ILP approach," *IEEE Trans. Power Del.*, vol. 23, no. 4, pp. 1812-1820, Oct. 2008.
- [28] "IEEE standard for synchrophasor measurements for power systems" in *IEEE Std C37.118.1-2011 (Revision of IEEE Std C37.118-2005)*, pp.1-61, Dec. 2011.
- [29] M. Brown, M. Biswal, S. Brahma, S. J. Ranade, and H. Cao, "Characterizing and quantifying noise in PMU data," in *Proc. IEEE Power & Energy Soc. General Meeting (PESGM)*, Boston, MA, pp. 1-5, Nov. 2016.
- [30] "IEEE Standard Requirements for Instrument Transformers" in *IEEE Std C57.13-2016*, pp. 1-96, Jan. 2016.
- [31] B. Azimian, R. Sen Biswas, A. Pal, and L. Tong, "Time synchronized state estimation for incompletely observed distribution systems using deep learning considering realistic measurement noise," accepted for presentation in *IEEE Power Eng. Soc. General Meeting*, 2021. [Online]. Available: <https://arxiv.org/ftp/arxiv/papers/2011/2011.04272.pdf>
- [32] M. Ghasemi Damavandi, V. Krishnamurthy, and J. R. Martí, "Robust meter placement for state estimation in active distribution systems," *IEEE Trans. Smart Grid*, vol. 6, no. 4, pp. 1972-1982, Jul. 2015.
- [33] "Resources | PES Test Feeder", *Site.ieee.org*, 2021. [Online]. Available: <https://site.ieee.org/pes-testfeeders/resources/>. [Accessed: 22-Feb-2021].
- [34] F. Bu, Y. Yuan, Z. Wang, K. Dehghanpour, and A. Kimber, "A time-series distribution test system based on real utility data," in *Proc. IEEE North American Power Symp. (NAPS)*, Wichita, KS, USA, 2019, pp. 1-6.
- [35] "OpenDSS", *SourceForge*, [Online]. Available: <http://sourceforge.net/projects/electricdss>. [Accessed: 22-Feb-2021].
- [36] D. A. Haughton, and G. T. Heydt, "A linear state estimation formulation for smart distribution systems," *IEEE Trans. Power Syst.*, vol. 28, no. 2, pp. 1187-1195, May 2013.
- [37] R. Sen Biswas, B. Azimian, and A. Pal, "A micro-PMU placement scheme for distribution systems considering practical constraints," in *Proc. IEEE Power Eng. Soc. General Meeting*, Montreal, Canada, pp. 1-5, 2-6 Aug. 2020.
- [38] K. Krishnamoorthy and T. Mathew, *Statistical tolerance regions: theory, applications, and computation*. Hoboken, N.J: Wiley, 2009.